Acta Geotechnica (2015) 10:643–650
DOI 10.1007/s11440-014-0326-z

RESEARCH PAPER

Hydromechanical model for internal erosion and its relationship with the stress transmitted by the finer soil fraction

Ricardo Moffat · Paulo Herrera

Received: 29 October 2013 / Accepted: 4 April 2014 / Published online: 15 June 2014

Abstract We present a theoretical model to determine the hydromechanical boundary of an internally unstable soil subject to vertical seepage. The model is based in momentum balance equations, which consider that the system is divided into three components: water, finer soil fraction, and coarser soil fraction. The parameters of the model are as follows: the effective stress, the porosity of the soil, the friction angle between the coarse and fine fractions, and the proportion of the effective stress that is transmitted to the finer fraction (G^*). Using laboratory data collected on a large permeameter, we demonstrate that the model is able to properly describe the observed behavior. Furthermore, we show that the value of G^* is related to the value of D_{15}'/d_{85}' proposed by Kezdi (Soil physics—selected topics. Elsevier, Amsterdam, 1979) and that it has the same trend as found experimentally by Skempton and Brogan (Geotechnique 44:449–460, 1994). The proposed model is a promising method to deduce an approximate value of critical hydraulic gradient that triggers internal erosion in a cohesionless soil of known particle size distribution curve.

Keywords Critical hydraulic gradient · Force transmission · Granular media · Internal instability · Suffosion

R. Moffat (✉) · P. Herrera
Department of Civil Engineering, University of Chile, Blanco Encalada 2002, Santiago, Chile
e-mail: rmoffatc@ing.uchile.cl

P. Herrera
e-mail: pherrera@ing.uchile.cl

1 Introduction

Seepage forces act on soil particles whenever there is a gradient of hydraulic head that generates water flow. These forces dangerously affect internally unstable soils as they may produce internal erosion or movement of the finer soil fraction. In this article, we consider that internal erosion occurs when particle migration yields a reduction in total volume and a consequent potential for collapse of the soil matrix as explained in Moffat et al. [13]. Internal instability is governed by (1) a geometric constraint and (2) a hydromechanical threshold. Hence, a soil that is deemed potentially unstable as a consequence of its gradation (geometric constrain) will exhibit particle migration when seepage-induced forces exceed a critical threshold or hydromechanical boundary, as observed in laboratory experiments [1, 14, 18] and numerical simulations [3, 4, 16].

Potential for development of internal instability is usually assessed using empirical methods such as those proposed by Kezdi [9] and Kenney and Lau [7, 8]. Kenney and Lau [8] defined a criterion based on the shape of the grading curve, defining a stability index $(H/F)_{\min}$, which represents a geometric constrain to the mobile fraction (finer fraction) particles through the skeleton or matrix of the soil (coarser fraction). A discrete envelope of points (H) is established for selected intervals of D to $4D$ on the grading curve (F) as shown in Fig. 1a. If the grading curve lies below a boundary defined initially by $H/F = 1.3$ over a portion of its finer end ($F < 0.2$ for soils with a primary fabric that is well graded soils, otherwise $F < 0.3$), it is deemed potentially unstable. Subsequent discussion of the approach [11, 15, 17] led to a reinterpretation of laboratory tests and a revised criterion given by $(H/F)_{\min} = 1$ [8].

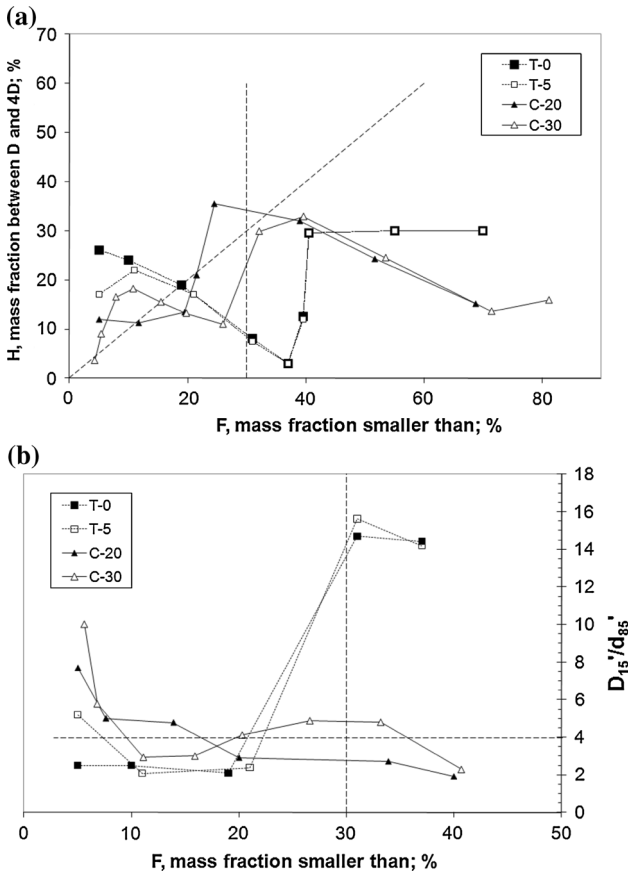

Fig. 1 Evaluation of internal stability: **a** after Kenney and Lau **b** after Kezdi (from [13])

On the other hand, a second criterion termed the filter ratio, which requires satisfying the ratio $D_{15}'/d_{85}' \leq 4$, was postulated by Kezdi [9] and independently conceived by de Mello [2]. It involves splitting the gradation at arbitrary points along the curve, to yield D_{15}' of the coarse fraction and d_{85}' of the fine fraction as shown in Figs. 1b and 2. The premise of this approach is that a potential for instability exists whenever $(D_{15}'/d_{85}')_{\max}$ exceeds 4, in accordance with the empirical criterion for base soil retention by a granular filter proposed by Terzaghi [20].

It is possible to establish the onset of instability defined as the critical hydraulic gradient (i_c), for which particle migration begins for a soil gradation considered potentially unstable according to the criteria explained above. For example, we can use test data for a single soil to estimate values of mean stress (σ') and local critical gradient (i_c) at the onset of internal instability. These values yield a hydromechanical envelope established experimentally by Moffat and Fannin [14] and shown in Fig. 3, which separates pairs of (i, σ') values into stable and unstable. This figure shows the average hydromechanical boundaries (in addition to minimum and maximum values) obtained experimentally for four different soils (T-0, T-5, C-20, and C-30). Above the hydromechanical boundary, the soil is expected to show internal erosion (unstable). In this paper, we will study whether a theoretical model can explain the hydromechanical boundaries observed experimentally.

The main objective of this study was to propose a simple theoretical model to estimate the critical hydraulic gradient that triggers the onset of internal instability from grading curve information of cohesionless soils. The proposed model considers that a fraction of the stress on the soil mass is transmitted to the finer fraction. Hereafter, grains with potential to move through the pore structure of a soil are referred to as fine or finer soil fraction. This finer fraction stress ratio is represented by the coefficient G^*, which we show to be proportional to the inverse value of D_{15}/d_{85} according to data from previously published laboratory tests [13, 14]. The proposed model should help to interpret laboratory data and to estimate the likelihood of internal erosion for expected hydraulic gradients in soils with known gradation.

2 Model formulation

A model based on porous media theory is developed and applied to support the concepts regarding the hydromechanical

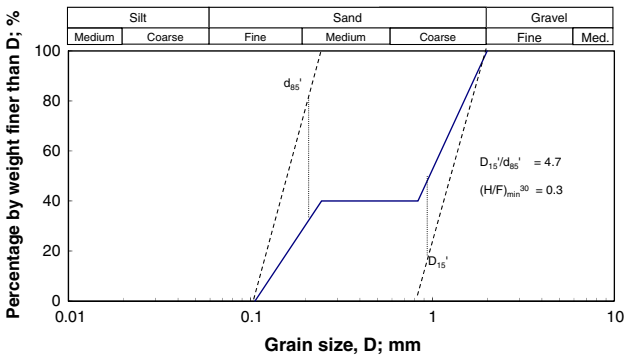

Fig. 2 Split gradation according to Kezdi's criterion [9]

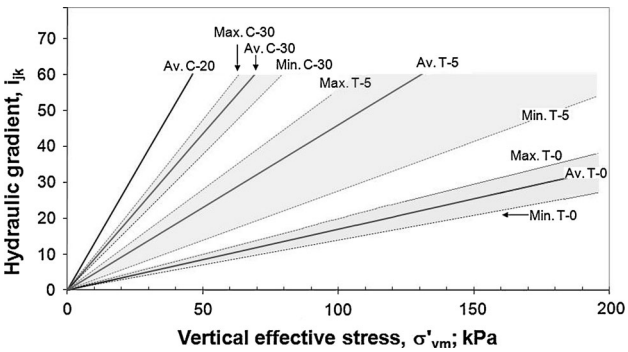

Fig. 3 Examples of hydromechanical boundaries for different soils (from [14])

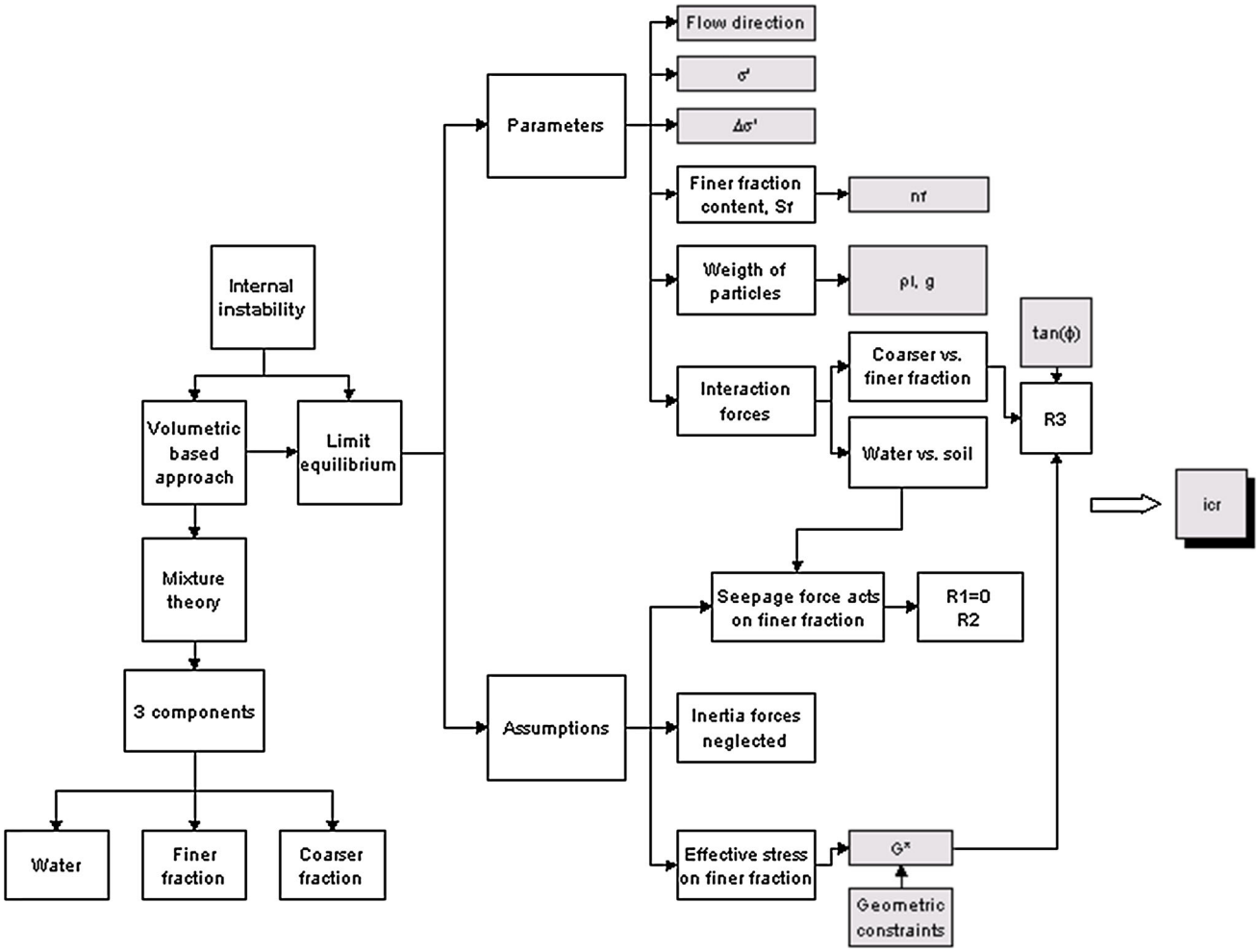

Fig. 4 Proposed model for internal instability

boundaries of internal instability, and to reconcile the apparent disconnect between geometric ranking and hydromechanical ranking as described by Moffat and Fannin [14]. A few studies have proposed physical models to determine the onset of internal particle migration in soils (e.g., [6, 19]. We propose a new model that considers the equilibrium of a three-component system that comprises water, soil skeleton, and finer fraction (mixture theory). The main features of this model are as follows: (1) the ability to include geometrical analysis based on the grain size distribution shape, (2) the capability of including the value of vertical effective stress and variation of vertical effective stress in the zone of failure, (3) it can be used to model downward or upward flow, considering the effect of gravity force, (4) includes strength parameters of the soil being tested such as friction angle, and (5) simplicity. The model can distinguish the general trend of hydromechanical boundaries for different materials and can be easily incorporated to a numerical code. This model is only applicable when the soil is potentially unstable according to Kezdi [9] or Kenney and Lau [7] and when the finer fraction content is below 35 %.

As shown in Figs. 4 and 5, the main assumptions of this model are as follows:

1. Inertial forces are neglected,
2. Seepage forces act mainly on the finer fraction particles
3. Effective stress on the finer fraction is a fraction of the total effective stress on the specimen.

Although, there is not much experimental evidence about the second assumption, it has been observed in numerical simulations that pressure gradients are much higher around finer soil particles due to the constriction of the pore space and the consequent change in permeability [3, 16]. Galindo-Torres et al. model solid particles of two different sizes observing that hydraulic gradient along the space occupied by the small particles is higher and forces increase in these particles due to the transfer of momentum from the fluid to the solid phase.

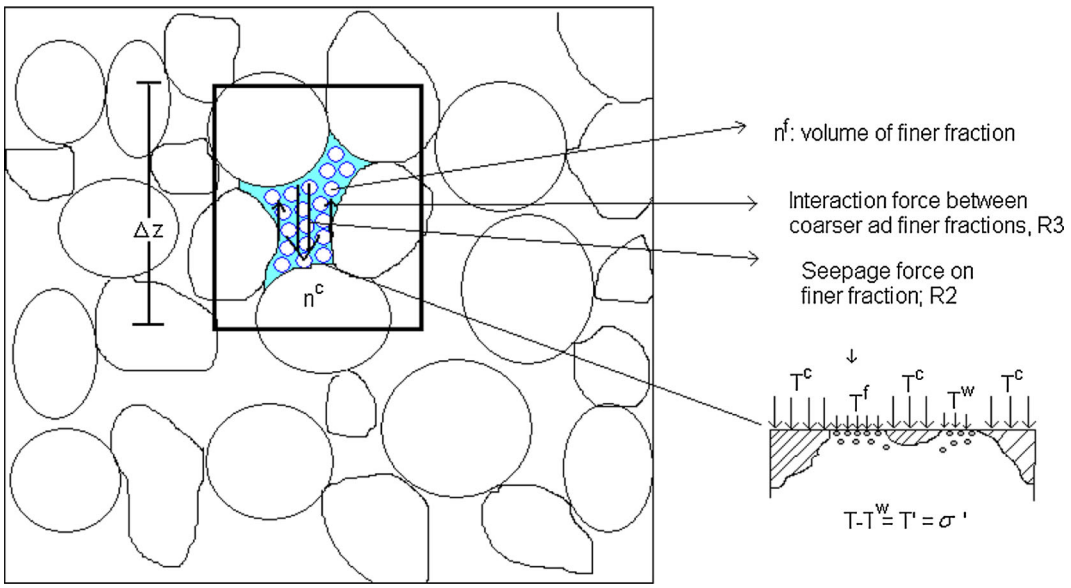

Fig. 5 Representative unit volume considered to derive the proposed theoretical model to estimate critical hydraulic gradients

Moffat et al. [13] and Moffat and Fannin [14] showed that different parameters influence the onset of internal instability. Therefore, the formulation of a physical model that is based on fundamental principles and that reflects the same characteristics observed during testing is extremely difficult.

For the formulation of our model, we start by considering a representative unit volume of soil that comprises three components that can move independently but that influence each other through interaction forces, as shown in Fig. 5 [5]. Then, the total stress over the soil volume is the sum of three components:

$$T = nT^{\mathrm{w}} + n^{\mathrm{c}}T^{\mathrm{c}} + n^{\mathrm{f}}T^{\mathrm{f}}$$

where T^{w} is the fraction of the total stress that is transmitted by water (pore water pressure), and T^{c} and T^{f} are partial stress on the coarse and finer fraction particles, respectively. Volumetric effects are considered through the use of n^{i} values that represent the volume fraction of each component.

Accordingly, the volume fractions of these components are as follows: $n^{\mathrm{w}} = n$: fluid (water) fraction, or porosity, n^{c}: coarser fraction volume ratio ($=1 - n - n^{\mathrm{f}}$), n^{f}: finer fraction volume ratio, where n^{f} is calculated as $n^{\mathrm{f}} = \frac{e}{S_{\mathrm{f}}} * 100$ [21, e: void ratio, and S_{f}: finer fraction content by mass (%).

Momentum balance can be used to describe the equilibrium limit of the three fractions. Vertical momentum balance of each component in the vertical direction is given by:

$$\frac{\partial T^{\mathrm{w}}}{\partial z} + \rho^{\mathrm{w}} g = R1 - R2 + \rho^{\mathrm{w}} \frac{\partial V_{\mathrm{w}}}{\partial t} : \text{water} \tag{1a}$$

$$\frac{\partial T^{\mathrm{c}}}{\partial z} + \rho^{\mathrm{c}} g = R3 - R1 + \rho^{\mathrm{c}} \frac{\partial V_{\mathrm{c}}}{\partial t} : \text{coarser fraction} \tag{1b}$$

$$\frac{\partial T^{\mathrm{f}}}{\partial z} + \rho^{\mathrm{f}} g = -R3 + R2 + \rho^{\mathrm{f}} \frac{\partial V_{\mathrm{f}}}{\partial t} : \text{finer fraction} \tag{1c}$$

where T^{i}: stress in the "i" component [M L/T^2/L^2], ρ^{i}: unit density of the "i" component ($\rho^{\mathrm{c}} = \rho^{\mathrm{f}} = 2.7$ mg/m^3; $\rho^{\mathrm{w}} = 1.0$ Mg/m^3), g: gravity [L/T^2], V_i: velocity of the "i" component [L/T], $R1$: interaction force water/coarser fraction [M L/T^2/L^2], $R2$: interaction force water/finer fraction [M L/T^2/L^2], $R3$: interaction force finer/coarser fraction [M L/T^2/L^2].

In the case of all the tests analyzed later, the increase in i_{av} is applied slowly to the soil, and therefore, the rate of change in seepage velocity can be considered very low or negligible ($(\frac{\partial V_w}{\partial t}) = 0$). Additionally, one can further simplify the model by assuming that the coarser and finer fractions do not move prior to the onset of instability. Therefore, inertial forces are neglected in this model, and the last term on the right-hand side of Eqs. 1a, 1b, 1c is equal to zero.

Consider now the interaction forces $R1$, $R2$, and $R3$ between the three components. $R1$ and $R2$ are function of the seepage force per unit volume, which can be approximated by $i \cdot \gamma_{\mathrm{w}}$ [20], where i is the local hydraulic gradient in the soil layer that is being analyzed. Further, it is assumed that due to the difference in size of the fine and coarse grains, the head loss occurs predominantly in the

finer fraction of the soil as its size is quite small compared to the coarser fraction. Thus, we can make an additional simplification and assume that seepage forces act entirely on the finer fraction, and therefore $R1 = 0$ and $R2 = i_{jk} \cdot \gamma_w$. $R3$, which corresponds to the interaction force per unit volume between the finer fraction and the coarser fraction of the soil, is calculated directly from Coulomb theory. Therefore, after replacing terms in Eqs. 1a, 1b, 1c, we obtain the following expression to calculate $R3$:

$$R3 = \frac{G^* \cdot \sigma'_{vm} \cdot \tan(\phi_\mu)}{n^f \Delta z}. \quad (2)$$

where Δz: unit length, G^*: geometric-based stress reduction factor, ϕ_μ: true friction angle between particles of the coarser and finer fraction.

In addition, we consider that the fine soil fraction transmits only a portion of the total effective stress (σ_{vm}') applied on the internally unstable specimen. The same hypothesis has previously been made by Skempton and Brogan [18], who believed that in sandy-gravel mixtures "the greater part of the overburden load is carried on a framework of primary fabric of gravel particles, leaving most of the sand under relatively small pressures." In fact, Skempton and Brogan [18] postulated that the framework or skeleton of gravel particles carried out a major portion of the effective stress, leaving the finer fraction of sand relatively unloaded. They hypothesized that the ratio between the effective stress on the finer portion and the effective stress on the coarser portion, called the stress reduction factor α, depends upon the grain size distribution curve. This hypothesis has also been verified through numerical simulations (e.g., [22]. In what follows, we assume that:

$$T^f = G^* \cdot \sigma'_{vm} \quad (3)$$

where G^* is a geometric-based factor that determines the proportion of stress transferred to the particles of the fine soil fraction (as does the value α introduced by Skempton and Brogan). Vertical effective stress σ_{vm}' has been used to relate to previous work of Skempton and Brogan and also Moffat and Fannin [14]. Mean stress could have been used and as the wall of the experiments are rigid, it would be proportional to the vertical stress in a factor related to the at rest coefficient of earth pressure (ko).

Then, approximating differential Eqs. 1a, 1b, 1c, 2, and 3, the critical hydraulic gradient i_{cr} can be estimated as:

$$i_{cr} = \frac{G^*}{\gamma_w \cdot \Delta z}\left(\sigma'_v \cdot \tan(\phi_\mu) + \Delta\sigma'_v\right) - \frac{n^f \rho_f g}{\gamma_w}$$
for downward flow (4a)

or

$$i_{cr} = \frac{G^*}{\gamma_w \cdot \Delta z}\left(\sigma'_v \cdot \tan(\phi_\mu) + \Delta\sigma'_v\right) + \frac{n^f \rho_f g}{\gamma_w}$$
for upward flow (4b)

Equation 4a, 4b suggests that the critical hydraulic gradient is a function of the effective stress on the soil specimen: As the effective stress increases, the value of i_{cr} also increases.

3 Application of proposed model to experimental data

Moffat and Fannin [14] analyzed data of permeameter tests performed with four different soil gradations and values of D_{15}'/d_{85}'. Table 1 summarizes the properties of these soils, and Table 2 contains values of i_{cr} and σ' at the onset of failure observed during those experiments. We also use the stress profiles deduced for each test to find the stress variation $\Delta\sigma_v'$ in the location where internal erosion began (see Table 2).

Additionally, the true friction angle between both fractions is estimated as $\phi_\mu = 35°$ for all the materials tested. While it is difficult to obtain a reliable evaluation of ϕ_μ [12], the assumed value of 35° is reasonable for bulky minerals such as a mix of quartz and feldspar.

We substitute the critical hydraulic gradient i_{cr} together with other parameters measured in the experiments performed by Moffat and Fannin [14] into Eqs. 4a, 4b. This procedure yields a value of G^* that is assumed unique for each soil and independent of the stress level, in the same way as Skempton and Brogan [18] assumed that the value α is unique for each soil.

Figures 6 and 7 show a comparison between the calculated values of i_{cr} and σ' at the onset of failure and the measured values in the laboratory. With a constant value of G^* for each soil, the model yields different hydromechanical boundaries for core and transition materials, which is consistent with results obtained experimentally.

Figure 8 shows that the estimated values of the geometric-based factor G^* become larger as the corresponding value of D_{15}'/d_{85}' gets smaller, resulting in greater values of i_{cr}. The main difference occurs when comparing core

Table 1 Characteristics properties and geometrical stability analysis of studied soils

Soil type	Fines content (% < 74 μm)	$(D_{15}'/d_{85}')_{max}$	$(H/F)^a_{min}$ $F < 0.2$
T-0	0	13.7 @ 30 %	0.95
T-5	5	14.3 @ 30 %	0.9
C-20	20	7.7 @ 5 %	0.67
C-30	30	10 @ 5.6 %	0.67

[a] Kenney and Lau method [8]

materials with transition materials. In contrast, the ratio D_{15}'/d_{85}' of T-0 and T-5 materials is very similar [14], and therefore, the value of G^* does not vary significantly. In addition, values of n^f are very similar for the two transition materials (see Table 2). Consequently, the difference in the slope of the hydromechanical boundary cannot be explained through geometric considerations alone, and the variation in effective stress $\Delta\sigma_{vm}'$ must be considered.

Additionally, values of α obtained by Skempton and Brogan [18] are also plotted on Fig. 8. It is possible to see that α values obtained independently in cohesionless internally unstable soils follow a similar trend than the values of G^* deduced from our model. We interpret this similarity as a validation of the proposed model.

4 Conclusions

We derived a physically based model to estimate the likelihood of internal instability for cohesionless soils and

Table 2 Parameters of experiments used to validate the proposed model

Test code	G^*	n^f	$\Delta\sigma_{vm}'$ (kPa)	Δz (m)	σ_{vm}' (kPa)	ϕ_μ	i_{cr} lab	i_{cr} model
T-0-25-D	0.145	0.269	2.5	0.125	38.1	35	7.0	7.9
T-0-100-D	0.145	0.279	12.6	0.125	62.1	35	12.2	9.1
T-0175-D	0.145	0.279	31.6	0.125	182.6	35	25.4	30.6
T-5-25-D	0.140	0.290	No failure			35		
T-5-175-U	0.140	0.290	64.5	0.125	101.1	35	58.4	49.2
T-5-50-D	0.140	0.287	−4.9	0.125	57.7	35	18.2	14.5
T-5-50-D (R)	0.140	0.289	−45.9	0.125	105.6	35	57.0	41.5
T-5-25-U	0.140	0.284	4.1	0.05	22.87	35	13.3	18.1
T-5-30-U	0.140	0.285	17.3	0.125	41.16	35	23.0	17.3
C-20-50-U	0.200	0.153	24.4	0.125	24.6	35	35.2	41.5
C-20-85-U	0.200	0.151	10.7	0.125	21.3	35	25.4	25.3
C-30-25-U	0.170	0.180	11.7	0.125	15.9	35	14.7	16.7
C-30-50-U	0.170	0.181	16.0	0.125	20.9	35	15.8	22.0
C-30-80-U	0.170	0.191	37.2	0.125	41.4	35	39.2	44.9
C-30-100-U	0.170	0.187	8.7	0.125	19.3	35	18.2	15.2
C-30-100-U	0.170	0.187	34.6	0.125	40.9	35	39.3	43.6

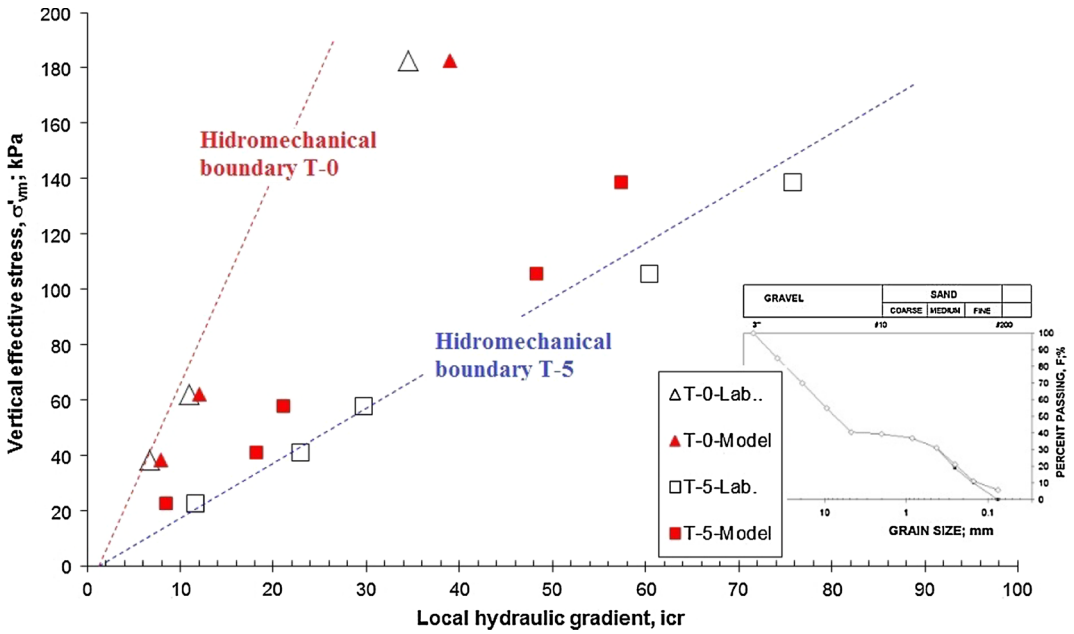

Fig. 6 Comparison of observed and estimated i_{cr} according to proposed model (Eqs. 4a, 4b) for transition materials

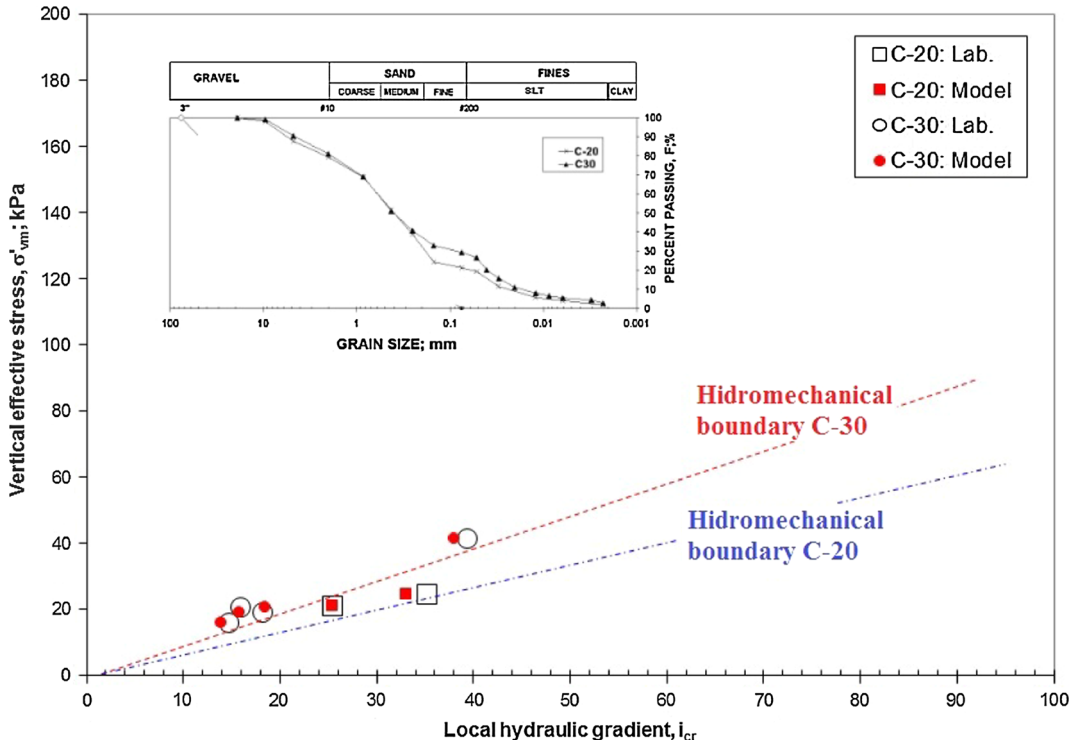

Fig. 7 Comparison of observed and estimated i_{cr} for core materials according to proposed model and experimental data (Eqs. 4a, 4b)

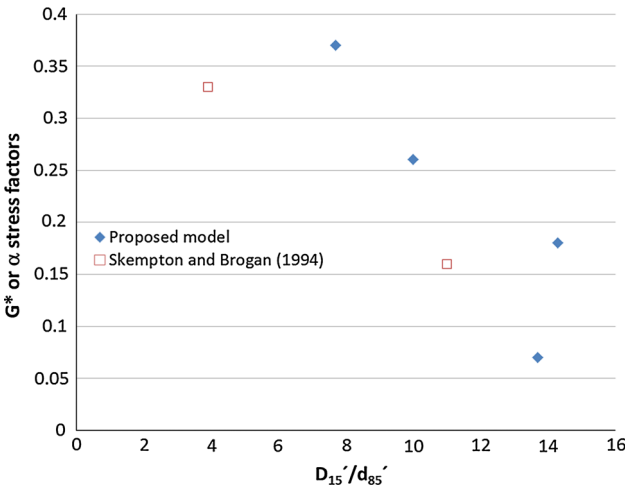

Fig. 8 Calculated geometric stress reduction factor G^* from experimental results according to Skempton and Brogan [18] and proposed model

applied it to analyze previously published experimental data [14]. The model was developed considering the interaction forces between three components: water, finer fraction, and coarser fraction; and three assumptions: inertial forces are neglected, effective stress on the finer fraction is a portion of the effective stress on the specimen, and seepage force acts only on the finer fraction particles.

Based on application of the proposed theoretical model to analyze experimental data for four widely graded cohesionless soils, we conclude that:

1. Effective stress and hydraulic gradient are deemed the most important parameters to define the onset of internal soil instability.
2. The model identifies and explains the importance of vertical effective stress variation ($\Delta\sigma_{vm}'$) in the direction of flow, in addition to the governing influence of mean vertical effective stress (σ_{vm}') and hydraulic gradient (i_{jk}) across the zone of failure.
3. The stress reduction factor G^* that defines the portion of the stress that is transmitted to the finer fraction of the soil decreases as the value of D_{15}'/d_{85}' increases. This means that for soils having values of $D_{15}'/d_{85}' > 4.0$ according to Kezdi [9], the critical hydraulic gradient i_{cr} becomes smaller under the same effective stress conditions in the soil for larger values of D_{15}'/d_{85}'.
4. Values of G^* are similar and follow the same trend as values of the parameter "α" previously found by Skempton and Brogan [18] in upward seepage tests with no external load applied to the soil simple.

Finally, we postulate that given a soil with known grain size distribution curve and effective stress distribution, it is possible to pick a corresponding value of G^* from Fig. 8 to

estimate using Eqs. 4a, 4b the critical hydraulic gradient i_{cr} that triggers internal instability. Hence, we expect that the proposed model will be a useful complement to existing criteria to assess the internal stability of soils in presence of water flow.

We envisage that in the future, the proposed model will be tested with results of additional laboratory experiments and through comparison with results of recently developed numerical models that are able to represent the coupled effect of mechanical and hydrodynamic forces on soil grains (e.g., [3, 4, 10].

Acknowledgments The authors acknowledge the comments of three anonymous reviewers which improved the original version of this manuscript.

References

1. Chang DS, Zhang LM (2011) A stress-controlled erosion apparatus for studying internal erosion in soils. Geotech Test J 34(6):579–589
2. De Mello FB (1975) Some lessons learned from unsuspected, real and fictitious problems in earth dam engineering in Brazil. In: Proceedings, 6th regional conference for Africa on soil mechanics and foundation engineering, Durban, South Africa, Sept 1975, pp 285–304
3. Galindo-Torres SA, Scheuermann A, Mühlhaus HB, Williams DJ (2013) A micro-mechanical approach for the study of contact erosion. Acta Geotech 1–12. doi:10.1007/s11440-013-0282-z
4. Han Y, Cundall PA (2013) LBM-DEM modeling of fluid–solid interaction in porous media. Int J Numer Anal Methods Geomech 37:1391–1407
5. Hassanizadeh M, Gray WG (1979) General conservation equations for multi-phase systems: 1. Averaging procedure. Adv Water Resour 2:131–144
6. Indraratna B, Radampola S (2002) Analysis of critical hydraulic gradient for particle movement in filtration. J Geotech Geoenviron 128:347–350
7. Kenney TC, Lau D (1985) Internal stability of granular filters. Can Geotech J 22:215–222
8. Kenney TC, Lau D (1986) Reply: internal stability of granular filters. Can Geotech J 23:420–423
9. Kezdi A (1979) Soil physics—selected topics. Elsevier, Amsterdam
10. Lominé F, Scholtès L, Sibille L, Poullain P (2013) Modeling of fluid–solid interaction in granular media with coupled lattice Boltzmann/discrete element methods: application to piping erosion. Int J Numer Anal Methods 37:577–596
11. Milligan V (1986) Internal stability of granular filters: discussion. Can Geotech J 23:414–418
12. Mitchell JK (1993) Fundamentals of soil behavior, 2nd edn. University of California, Berkeley. John Wiley & Sons, Inc.
13. Moffat R, Fannin RJ, Garner SJ (2011) Spatial and temporal progression of internal erosion in cohesionless soils. Can Geotech J 48:1–14
14. Moffat R, Fannin RJ (2011) A hydromechanical relation governing the internal stability of cohesionless soils. Can Geotech J 48:1–12
15. Ripley CF (1986) Internal stability of granular filters: discussion. Can Geotech J 23:255–258
16. Sari H, Chareyre B, Catalano E, Philippe P, Vincens E (2011) Investigation of internal erosion processes using a coupled DEM-fluid method. In: Oate E, Owen DRJ (eds) Particles 2011 II international conference on particle-based methods, Barcelona
17. Sherard JL, Dunnigan LP (1986) Internal stability of granular filters: discussion. Can Geotech J 23:418–420
18. Skempton AW, Brogan JM (1994) Experiments on piping in sandy gravels. Geotechnique 44:449–460
19. Shire T, O'Sullivan C (2013) Micromechanical assessment of an internal stability criterion. Acta Geotech 8:81–90
20. Terzaghi K (1939) "Soil mechanics: a new chapter in engineering practice". 45th James Forrest lecture. J Inst Civ Eng 12:106–142
21. Thevanayagam S (1998) Effects of fines and confining stress on undrained shear strength of silty sands. J Geotech Geoenviron 123:479–490
22. Voivret C, Radjai F, Delenne J-Y, El Youssou MS (2009) Multiscale force networks in highly polydisperse granular media. Phys Rev Lett 102:178001